Sustainable Food Technology

ROYAL SOCIETY OF CHEMISTRY

PAPER

View Article Online
View Journal

Cite this: DOI: 10.1039/d6fb00033a

Preparation and characterization of pH-responsive fucoidan/carboxymethyl chitosan hydrogel beads for curcumin encapsulation and *in vitro* gastrointestinal release

Jiayu Yu,[a] Hongyang Hu,[a] Yingyi Wang,[a] Xia Sun,[a] Hanxu Li,[a] Shun Xiao,[a] Bingcan Chen *[b] and Hui Li*[a]

Curcumin (Cur) features versatile bioactivities but suffers from poor stability and high vulnerability to gastrointestinal degradation. To address these bottlenecks, an effective and facile strategy for constructing a sustainable hydrogel delivery system with pH-responsive function and controlled gastrointestinal release properties is reported. The hydrogel beads were developed through physical crosslinking between fucoidan (Fuc), carboxymethyl chitosan (CMCS), and the encapsulated bioactive compound Cur. Structural characterization confirmed that intermolecular hydrogen bonding between Fuc and CMCS played a pivotal role in the hydrogel network formation. Cur was efficiently encapsulated within the hydrogel beads, functioning as an additional crosslinking agent that increased the crosslinking density and reduced the equilibrium water content of the system. Notably, the hydrogel beads protected Cur *via* non-covalent interactions and physical barriers, enhancing its thermal and UV stabilities. Furthermore, the hydrogel beads exhibited pronounced pH-responsive swelling and release behaviors, showing minimal swelling and limited release under acidic gastric conditions, in contrast to sharp swelling and near-complete release in alkaline intestinal environments, attributed to the pH-dependent protonation states of polysaccharides' functional groups altering intermolecular interactions. Importantly, the encapsulated Cur retained more than 90% antioxidant capacity following simulated gastrointestinal digestion. This crosslinker-free and food-grade system provides a safe delivery platform for labile polyphenols, showing considerable potential in functional foods and dietary supplements.

Received 2nd February 2026
Accepted 24th May 2026

DOI: 10.1039/d6fb00033a

rsc.li/susfoodtech

Sustainability spotlight

This study supports sustainability by constructing a pH-responsive fucoidan/carboxymethyl chitosan hydrogel beads for the encapsulation of bioactive curcumin. An innovative and environmentally friendly strategy was developed for the fabrication of the hydrogel beads solely relying on one hydrogen bonding among the protonated sulfate groups of fucoidan, the carboxyl groups of carboxymethyl chitosan hydrogel, and the hydroxyl groups of curcumin under acidic conditions, thereby eliminating the need for chemical modifiers. The strategy exploits the intrinsic functional groups of readily available food biopolymers and bioactive compounds to enable a practical and green strategy for the encapsulation of other natural phenolic compounds.

1 Introduction

With the rising consumer demand for functional foods that integrate nutrition and health benefits, the food industry has increasingly focused on incorporating food-derived bioactive compounds (*e.g.*, polyphenols, vitamins, and bioactive lipids) into daily products. Curcumin (Cur), a natural polyphenol derived from *Curcuma longa* L., has attracted extensive attention in food science and nutrition owing to its versatile bioactivities, including antioxidant, anti-inflammatory, gut-protective, and chronic disease-mitigating properties.[1] However, the direct utilization of Cur in food systems is severely hindered by inherent physicochemical limitations, such as extremely low water solubility, poor chemical stability, and rapid degradation in the gastrointestinal tract (GIT),[2] which collectively result in low bioavailability and compromised functional efficacy. Hence, addressing these challenges is critical for unlocking the full application potential of Cur in formulating it into the existing food products.

To overcome the delivery bottlenecks of Cur, various encapsulation systems have been developed over the past decades, such as lipid-based carriers, protein-based matrices, polymeric nanoparticles, and microcapsules.[3,4] Despite the fact

[a]College of Food Science and Engineering, Jilin University, Changchun, Jilin, 130062, China. E-mail: lihuiqq23@jlu.edu.cn
[b]Department of Plant Sciences, North Dakota State University, Fargo, ND 58108, USA. E-mail: bingcan.chen@ndsu.edu

that these systems have shown certain effects in improving the stability and bioavailability of Cur, they share inherent limitations, such as the susceptibility to lipid oxidation, high sensitivity to pH, temperature, and enzymatic degradation.[5] Hence, there remains an urgent need to develop a biocompatible, stable, and cost-effective delivery system that can efficiently protect Cur during food processing and after ingestion.

Food biopolymer based hydrogels are three-dimensional network materials formed by polysaccharides and/or proteins in aqueous microenvironments, whose tunable physicochemical properties enable responsiveness to environmental stimuli.[6] Specifically, their pH-sensitivity has attracted significant attention for oral food applications, as they can adapt to the distinct pH gradients of the GIT.[7] Such systems protect bioactive compounds in acidic gastric environments while triggering release in the intestine *via* pH-responsive mechanisms. Fucoidan (Fuc), a sulfated polysaccharide rich in sulfate groups from brown algae, exhibits diverse bioactivities, including antioxidant, anti-tumor, immunomodulatory, and antithrombotic activities.[8,9] The sulfate groups in the Fuc chain undergo pH-dependent protonation/deprotonation (pK_a 1.0–2.5) and endow correspondingly gastric pH responsiveness.[10] Carboxymethyl chitosan (CMCS) is a versatile chitosan derivative containing adequate amino and carboxyl groups and combines chitosan's biocompatibility with superior water solubility and pK_a values of 6.5 and 2.7 within the gastrointestinal pH range.[11,12] Importantly, CMCS's anionic nature enables miscibility with Fuc in aqueous solutions which avoids the development of insoluble polyelectrolyte complexes.[11] Despite the favorable properties of Fuc and CMCS, Fuc alone lacks sufficient gelling ability, limiting its direct application in hydrogel fabrication.[13] Therefore, certain chemical crosslinking strategies such as aldehyde modification of Fuc or EDC/NHS coupling have been reported to prepare Fuc–CMCS hydrogels.[14,15] However, these chemical approaches involve toxic reagents, complicated modification procedures, and potential food safety risks, which violate the principles of green and sustainable food processing. Additionally, such conventional methods overlook the presence of abundant hydroxyl and sulfate groups in Fuc as well as the carboxyl, amino, and hydroxyl groups in CMCS, which may potentially provide abundant sites for intermolecular hydrogen bond interactions and facilitate the assembly of stable composite hydrogels without the need for chemical modifications.

Building on the complementary structural features and hydrogen bond-forming capacities of Fuc and CMCS, we hypothesize that simple, green, hydrogen bond-mediated Fuc/CMCS composite hydrogel beads can effectively resolve the delivery bottlenecks of Cur. Inspired by the strong binding affinity between polyphenols and dietary polysaccharides *via* non-covalent interactions in natural plant cell walls,[16] this composite hydrogel system is expected to efficiently encapsulate and stabilize Cur *via* hydrogen bonds formed between the phenolic hydroxyl groups of Cur and the functional groups of Fuc and CMCS. Furthermore, the hydrogen bond-crosslinked Fuc/CMCS network will exhibit inherent pH responsiveness, as changes in GIT pH alter the stability of intermolecular interactions, thereby protecting Cur in the stomach and triggering its controlled release in the intestine.

Hence, this study designed and fabricated hydrogen bond-mediated physically crosslinked Fuc–CMCS hydrogel beads for Cur encapsulation. The physicochemical structure, swelling behaviors, pH responsiveness and mechanism, the stability of Cur under various conditions, and the corresponding release profiles of Cur from the hydrogel beads were thoroughly explored. Meanwhile, the free radical scavenging ability, monitored by real-time electron paramagnetic resonance (EPR) spectroscopy, was evaluated after *in vitro* simulated gastrointestinal digestion to assess both the antioxidant capacity of encapsulated Cur and the protective mechanism of the hydrogel beads. This green, chemically unmodified design developed in this study follows sustainable food processing guidelines and provides a safe platform for stabilizing and delivering labile bioactive compounds, with considerable potential in functional foods and dietary supplements.

2 Materials and methods

2.1 Materials

Fuc (from: brown seaweed, purity: 98%, sulphation degree: 0.24, molecular weight: 121.6 kDa) was purchased from Macklin Biochemical Technology Co., Ltd (Shanghai, China). CMCS (carboxylation degree: ≥80%, deacetylation degree: 88–92%, molecular weight: 100 kDa), Cur, polyethylene glycol 400 (PEG400), and 1,1-diphenyl-2-picrylhydrazyl (DPPH) were supplied by Aladdin Biochemical Technology Co., Ltd (Shanghai, China). Trypsin (from porcine pancreas), pepsin (pig source), and bile salt (pig source) were supplied by Macklin Biochemical Technology Co., Ltd (Shanghai, China).

2.2 Preparation of Fuc–CMCS@Cur hydrogel beads

Specifically, Fuc and CMCS were separately dissolved in deionized water to prepare polysaccharide solutions with a concentration of 5% (w/v). A 0.5 mg per mL Cur solution was prepared by dissolving in a PEG400/deionized water mixture with a volume ratio of 1 : 3. PEG400, an FDA approved food-grade polymer, served to enhance the dispersibility of Cur in deionized water, thereby facilitating the uniform dispersion of Cur within the hydrogel matrix.[17] To prepare Cur-encapsulated hydrogel beads, the Cur stock solution was thoroughly blended with equal volumes of Fuc and CMCS solutions under gentle stirring to ensure homogeneous mixing. The obtained mixed solution was then slowly and carefully added dropwise into 0.1 M HCl solution using a 10 μL pipette tip to induce gelation and bead formation. The reaction was allowed to proceed for 1 h to ensure complete crosslinking, even though the hydrogel beads formed instantaneously. Finally, the as-prepared hydrogel beads (denoted as Fuc–CMCS@Cur) were collected and washed three times with deionized water to remove residual surface components, and then used for subsequent characterization and analysis. A control of mixed Fuc and CMCS was prepared following the same procedure but replacing the Cur with the same volume of deionized water.

2.3 Encapsulation efficiency (EE) and loading capacity (LC)

To evaluate the EE and LC of the hydrogel bead system, the prepared hydrogel beads were transferred to ethanol to extract Cur with the assistance of ultrasound. Subsequently, the insoluble polysaccharides were precipitated by centrifugation (12 000 rpm, 2 min), and the supernatant was carefully collected. The concentration of Cur in the supernatant was measured by recording the absorbance at 426 nm using a UV-vis spectrophotometer. The amount of encapsulated Cur was determined by referring to a standard curve. The Cur-encapsulated hydrogel beads were then freeze-dried for LC determination. EE and LC were calculated using the following equations:

$$\text{EE (\%)} = \text{mass of encapsulated Cur/mass of added Cur} \times 100\%$$

$$\text{LC (\%)} = \text{mass of encapsulated Cur/(mass of beads + mass of encapsulated Cur)} \times 100\%$$

2.4 Structural characterization

Fourier transform infrared (FTIR) spectra of the samples were recorded ranging from 4000 to 400 cm^{-1} using an FTIR spectrometer (BRUKER Vertex 70) equipped with an attenuated total reflectance (ATR) module. The spectra were obtained by accumulating 32 scans at a resolution of 4 cm^{-1}. X-ray diffraction (XRD) data were obtained using an X-ray powder diffractometer (BRUKER D8 ADVANCE) with a voltage of 40 kV and a current of 40 mA, utilizing Cu Kα radiation ($\lambda = 1.5406$ Å). The samples were scanned over a diffraction angle 2θ range from 5 to 50° at a scanning rate of 5° min^{-1}. Thermogravimetric analysis (TGA) was performed using a TA Instruments Q50 thermogravimetric analyzer under a nitrogen atmosphere with a flow rate of 30 mL min^{-1}. The samples were placed in an alumina crucible and heated from 30 to 600 °C at a heating rate of 10 °C min^{-1}. A scanning electron microscope (SEM, Zeiss-Merlin Gemini SEM 300) was used to observe the surface and cross-sectional morphologies of freeze-dried samples at an acceleration voltage of 5 kV. UV-vis absorption spectroscopy was conducted ranging from 250 to 550 nm by using a PerkinElmer Lambda 35 UV-vis spectrophotometer. The samples were placed in a 10 mm path length quartz cuvette for the measurement.

2.5 Thermal and UV stabilities

Free Cur solution and Fuc–CMCS@Cur hydrogel beads with equal weight of Cur were subjected to different treatments. They were placed in the dark at 4, 20, 37, 60, and 80 °C for 1 h, or in the dark at 80 °C for 3 h, or under 365 nm UV irradiation for 3 h. Subsequently, the absorbance of the solutions was measured at 426 nm using a UV-vis spectrophotometer to assess the retention of Cur in the samples. The Cur retention rate was calculated using the following formula:

$$\text{Cur retention rate (\%)} = \text{mass of Cur in treated samples under different conditions/mass of Cur in untreated samples} \times 100\%$$

2.6 Measurement of the pH-sensitive swelling behavior

Equilibrium water content (EWC) of hydrogel beads was determined as follows.[18] The samples were soaked in deionized water at room temperature to achieve their equilibrium swelling. The weight of swollen hydrogel beads is denoted as W_s. Subsequently, these swollen hydrogel beads were freeze-dried and weighed as W_d. The EWC was calculated according to the following equation:

$$\text{EWC (\%)} = (W_s - W_d)/W_d \times 100\%$$

The swelling behavior of the hydrogel beads was investigated by a weighing method. Briefly, the freeze-dried samples were accurately weighed and designated as M_1. These samples were then placed in separate Petri dishes, each containing an equal volume of medium solutions with varying pH values (2.0, 4.0, 6.0, and 7.4). After 4 h, the swollen samples were carefully taken out from the solutions. Excess liquid on the surface of the samples was gently blotted off using filter paper, and the samples were subsequently weighed as M_2. The swelling degree was calculated using the following formula:

$$\text{Swelling degree (\%)} = (M_2 - M_1)/M_1 \times 100\%$$

The size of swollen hydrogel beads was determined using particle sizing analysis software, and the mean size change rate was calculated using the following equation:

$$\text{Mean size change rate (\%)} = (D_s - D_{fd})/D_{fd} \times 100\%$$

where D_s represents the mean size of swollen hydrogel beads and D_{fd} represents the mean size of freeze-dried hydrogel beads.

2.7 Measurement of the pH-sensitive release behavior

The pH-sensitivity of the hydrogel beads was evaluated by studying the release profile of Cur from the hydrogel beads in medium solutions with different pH values (2.0, 4.0, 6.0, and 7.4). Specifically, the Fuc–CMCS@Cur hydrogel beads were separately incubated in various pH-adjusted medium solutions for 4 h. At 30 minute intervals, 0.1 mL of the supernatant was withdrawn for Cur determination and immediately replaced with fresh medium to maintain constant volume. The withdrawn supernatant was then mixed with 0.9 mL of ethanol. The absorbance of Cur in the supernatant was measured at 426 nm using a UV-vis spectrophotometer.

2.8 *In vitro* simulated gastrointestinal environment release

The simulated gastric fluids (SGFs, pH 2.0) and simulated intestinal fluids (SIFs, pH 7.0) were prepared according to the methods with some modification.[19] Briefly, SGF was prepared by adjusting a 0.2% (w/v) NaCl solution to pH 2.0 with a 1.0 M HCl solution. A specific amount of gastric protease was added to the solution to achieve a final concentration of 3.0% (w/v). For the SIF, trypsin and bile salt were evenly dispersed in a PBS buffer

(pH 7.0) with final concentrations of 1.0% and 0.8% (w/v), respectively. Subsequently, the pH value of the mixture was adjusted to 7.0 using a 1.0 M NaOH solution.

To investigate the release profile of Cur from the hydrogel beads, the Fuc–CMCS@Cur hydrogel beads were initially incubated in the SGF at 37 °C for 2 h. After that, the hydrogel beads were transferred to the SIF and maintained at 37 °C for 4 h. At 30 minute intervals, 0.1 mL of the supernatant was withdrawn for the determination of Cur and replaced with fresh medium to keep the volume constant. The withdrawn supernatant was mixed with 0.9 mL of ethanol, and the absorbance of Cur in the supernatant was measured at 426 nm using a UV-vis spectrophotometer.

2.9 DPPH radical scavenging capacity test

The DPPH radical scavenging capacity of samples was determined by electron paramagnetic resonance (EPR) spectroscopy. In detail, the hydrogel beads that had been digested by either SGF (2 h) or SIF (4 h) were mixed with an equal volume of 0.2 mM DPPH ethanol solution. Immediately after mixing, the EPR signal of DPPH was monitored. The hydrogel beads incubated in PBS (pH 7.4) served as the control group. The double-integration of the EPR spectrum, commonly known as the EPR signal, was then used to determine the extent of DPPH reduction according to the following formula:[20]

$$\text{EPR signal reduction (\%)} = (S_{\text{DPPH}} - S_{\text{sample}})/S_{\text{DPPH}} \times 100\%$$

where S_{DPPH} represents the EPR signals for free DPPH ethanol solution and S_{sample} represents the EPR signals of hydrogel beads.

The antioxidant kinetic process of hydrogel beads was determined by single exponential or biexponential fitting kinetic parameters using the following formula:[20]

$$\text{EPR}_{\text{signal}} = S_0 + A\exp(-(t - t_0)/t_1)$$

$$\text{EPR}_{\text{signal}} = S_0 + A\exp(-(t - t_0)/t_1) + B\exp(-(t - t_0)/t_2)$$

where EPR signal denotes the double integration of the DPPH scavenging EPR spectrum along time, while t_1 and t_2 correspond to the time constants for the DPPH decay of two different antioxidant processes, respectively.

2.10 Statistical analysis

All experiments were performed in triplicate and results were analyzed using IBM SPSS software. One-way ANOVA with Tukey test was applied for significance tests, and differences were considered significant if $p < 0.05$.

3 Results and discussion

3.1 Preparation of Fuc–CMCS and Fuc–CMCS@Cur hydrogel beads

As expected, individual biopolymer solutions (pure Fuc or CMCS) could not form hydrogel beads under our experimental conditions. Interestingly, we observed that hydrogel beads were able to form by mixing Fuc and CMCS solutions in an acidic environment. In order to better compare the effect of Cur on the properties of the hydrogel beads formed from Fuc and CMCS, we first optimized the volume ratio of the Fuc and CMCS mixture. To do so, the mixed solution of Fuc and CMCS with various volume ratios (3 : 1, 2 : 1, 1 : 1, 1 : 2, 1 : 3) was injected dropwise into a 0.1 M HCl solution to prepare hydrogel beads. As shown in Fig. 1a, the fabricated hydrogel beads displayed characteristic spherical morphology with uniform white color and were dependent on Fuc/CMCS volume ratios. Specifically, a concentration-dependent morphological alteration was observed with the increase of Fuc content, manifested by progressive opacity enhancement, measurable size reduction, and pronounced tailing formation, suggesting the gradual densification of the three-dimensional polymeric network structure. Meanwhile, extreme mixing volume ratios (Fuc/CMCS $\geq$ 3 : 1 or $\leq$1 : 3) could not produce stable spherical architecture. This phenomenon stemmed from competitive hydrogen bonding interactions in the Fuc/CMCS/water system where individual polysaccharide (Fuc or CMCS) preferentially engaged in hydration with water molecules rather than forming interpolymer crosslinks, resulting in failure to form a three-dimensional network structure. Accordingly, a Fuc/CMCS volume ratio of 1 : 1 was selected to prepare the optimized control sample (Fuc–CMCS) as well as the Cur-encapsulated hydrogel beads (Fuc–CMCS@Cur) following the identical procedure as described in Section 2.2 and illustrated in Fig. 1b. Regarding the appearance of Fuc–CMCS@Cur, no other notable alterations were observed except the unmistakable yellow color of the hydrogel beads (Fig. 1b). The encapsulation efficiency (EE) and loading capacity (LC) of the hydrogel beads for Cur were determined to be 88.22% and 3.45 mg g^{-1}, respectively. The high EE value could be ascribed to the strong intermolecular hydrogen bonding interactions between Cur and the Fuc–CMCS polysaccharide network, which effectively trapped Cur molecules inside the hydrogel matrix during the acidic gelation process. Meanwhile, the considerable LC value indicated that the hydrogel beads exhibited favorable loading potential for hydrophobic Cur, wherein food-grade PEG400 promoted Cur uniform dispersion and facilitated its homogeneous integration into the hydrogel network.

3.2 Characterization of Fuc–CMCS hydrogel beads and Fuc–CMCS@Cur hydrogel beads

3.2.1 Structural and physical properties. Given that FTIR can evaluate the interactions among different components within composite hydrogel beads, the FTIR spectra of Fuc, CMCS, Cur, Fuc–CMCS, and Fuc–CMCS@Cur hydrogel beads were determined (Fig. 2a). The FTIR spectra of Fuc, CMCS, and Cur exhibited broad absorption peaks in the range of 3000–3600 cm^{-1}, corresponding to the –OH stretching vibration. Additionally, a characteristic peak observed at approximately 2800 cm^{-1} was assigned to C–H stretching vibrations.[21] For Fuc, the absorption peak at 1616 cm^{-1} was associated with the presence of 2-*O*-acetyl groups in the structure. A broad band in the range of 1222–1260 cm^{-1} corresponded to the stretching

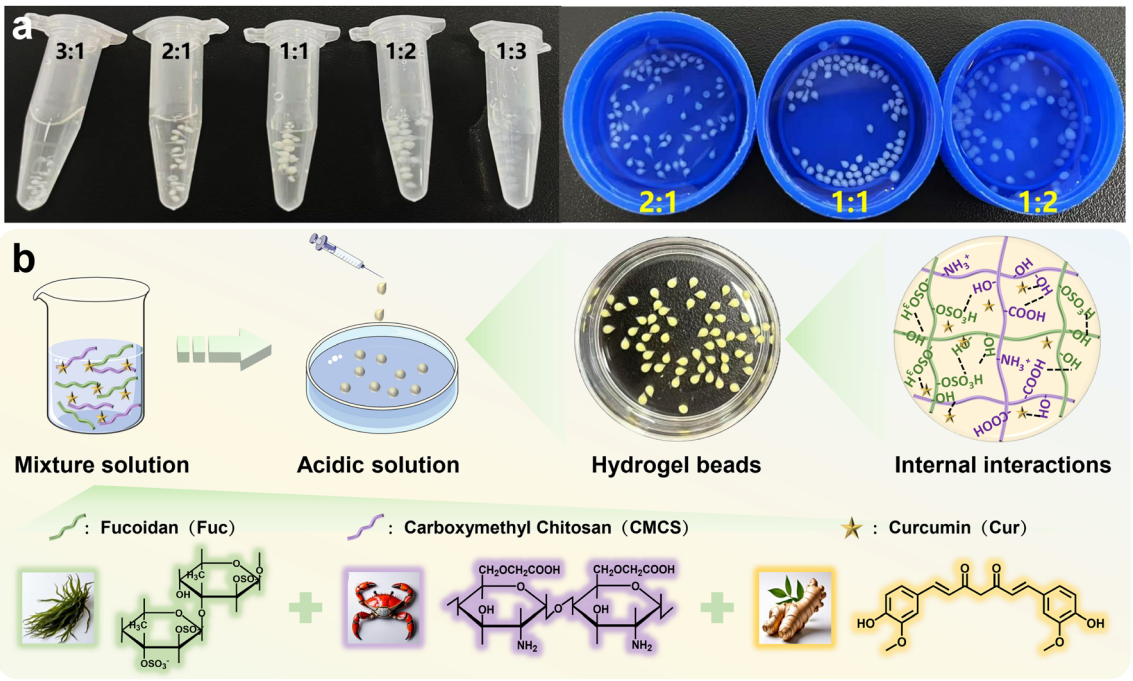

Fig. 1 (a) Digital photographs of the freshly prepared hydrogel beads with various volume ratios of Fuc/CMCS; and (b) schematic diagram for the preparation and crosslinking mechanism of Fuc–CMCS@Cur hydrogel beads.

vibration of S=O, and the absorption peak at 838 cm^{-1} was related to the stretching vibration of C–O–S.[22] For CMCS, a broad absorption peak at 3000–3600 cm^{-1} was also assigned to stretching vibrations of N–H. The characteristic peaks at 1582 and 1409 cm^{-1} originated from the asymmetric and symmetric stretching vibrations of $-COO^-$.[23] By contrast, the spectra of Fuc–CMCS and Fuc–CMCS@Cur hydrogel beads showed several significant alterations. A new peak appeared at 1211 cm^{-1} potentially attributed to the protonation of $-NH_2$ groups within the CMCS chain.[24] Moreover, the newly observed characteristic peak at 1731 cm^{-1} (Fig. 2b) corresponded to the protonated carboxyl groups (–COOH) in CMCS.[25] These protonated functional groups could readily form intermolecular hydrogen bonding interactions with the –OH groups present in both Fuc and Cur. The characteristic absorption peak at 838 cm^{-1}, assigned to the C–O–S stretching vibration of sulfate groups in Fuc, exhibited a noticeable shift to 836 cm^{-1} after hydrogel bead formation (Fig. 2b).[26,27] According to previous reports, this shift was typically induced by hydrogen bond formation between sulfate groups in Fuc and hydroxyl groups in CMCS and Cur.[10] Furthermore, the broad absorption band associated with –OH stretching was shifted from 3378 cm^{-1} in Fuc–CMCS to 3375 cm^{-1} in Fuc–CMCS@Cur. This change further confirmed the formation of hydrogen bonding interactions between Cur and the Fuc–CMCS polysaccharide network,[28] collectively demonstrating that Cur was successfully encapsulated within the hydrogel beads. The significant overlap between the main absorption bands of Cur and those of polysaccharides, coupled with the low content of Cur, likely accounted for the minimal alterations observed in the FTIR after Cur encapsulation.[29]

XRD was employed to investigate the crystal or amorphous structural changes of the hydrogel bead matrix and Cur (Fig. 2c). The characteristic broad diffraction peaks of Fuc and CMCS were found at $2\theta = 22.8°$ and 20.2°, respectively, indicating their amorphous state. The XRD diffraction patterns of Fuc–CMCS and Fuc–CMCS@Cur hydrogel beads exhibited even broader and weaker peaks in the same angular region. This transformation primarily resulted from competitive hydrogen bonding interactions between Fuc and CMCS, specifically disrupting the formation of individual hydrogen bonds and altering the crystalline region of polysaccharides.[30] Notably, free Cur manifested a distinguishable crystalline structure. However, for Fuc–CMCS@Cur hydrogel beads, the characteristic diffraction peaks of free Cur disappeared entirely, which was probably attributed to the intermolecular interactions that took place between Cur and polysaccharide matrix during the encapsulation procedure. Such interactions led to the obscuration or alteration of the molecular arrangement of Cur upon encapsulation. Consequently, there was a transition of Cur from a crystalline state to an amorphous state.[31]

The thermal properties of Cur, polysaccharides, and the formed hydrogel beads were assessed using TGA (Fig. 2d). In the case of pure Fuc and CMCS, the first stage degradation occurred within a temperature range of approximately 30–220 °C, which was mainly caused by the diffusion loss of free water and bound water within Fuc and CMCS, accompanied by the partial cleavage of glycosidic bonds.[32] The second stage corresponded to a temperature range of 220–340 °C, and was predominantly characterized by the cleavage of glycosidic bonds presented within the structural units of Fuc and CMCS. Moreover, during this particular stage, adjacent hydroxyl groups were eliminated

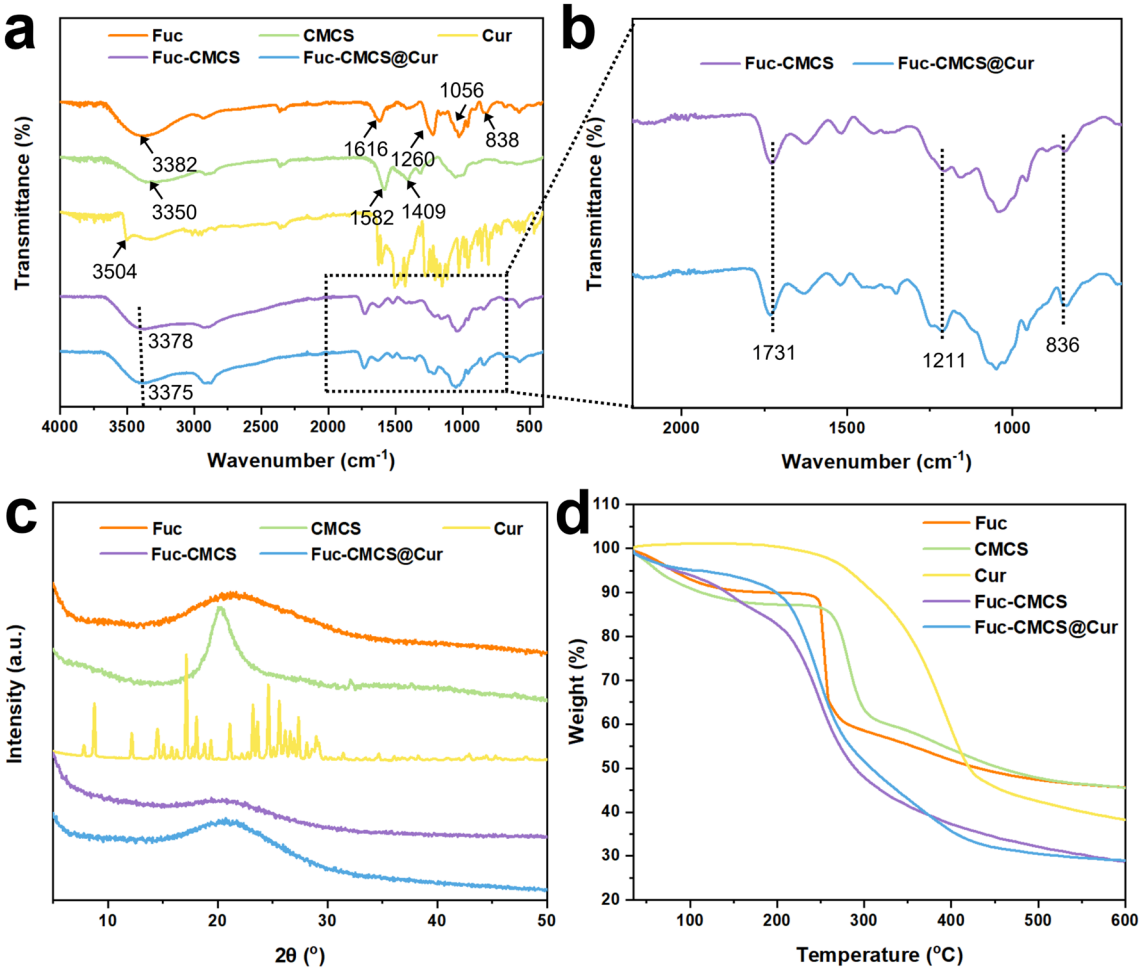

Fig. 2 (a) Raw and (b) enlarged FTIR spectra, (c) XRD patterns, and (d) TGA thermograms of Fuc, CMCS, Cur, Fuc–CMCS hydrogel beads and Fuc–CMCS@Cur hydrogel beads.

in the form of water molecules, and eventually, the intermediate products experienced carbonization and decomposition. Conversely, the thermal decomposition patterns of the hydrogel beads exhibited markedly distinct characteristics compared to the individual components. The initial degradation of the hydrogel beads was primarily caused by the loss of free water and bound water within the temperature range of 30–190 °C. At 190 °C, Fuc–CMCS exhibited 15.87% weight loss when compared to 8.90% for Fuc–CMCS@Cur, indicating that the latter contained less water. This phenomenon was likely due to the addition of Cur, which weakened the interaction between the polysaccharide matrix and water, thereby reducing available sites for water coordination. Subsequently, the notable weight loss in the temperature range of 190–350 °C could be ascribed to the disruption of polysaccharide intramolecular and intermolecular interactions, caused by the depolymerization of molecular rings along with the cleavage of saccharide rings and glycosidic bonds.[32] The weight loss of Fuc–CMCS@Cur hydrogel beads at 350–430 °C was probably due to the decomposition of Cur, as evidenced by the curve of free Cur. Finally, the hydrogel beads' matrix underwent gradual thermal decomposition at a higher temperature of 430–600 °C.[33]

3.2.2 Morphology and microstructure. The surface and cross-sectional morphologies, as well as microstructures of lyophilized Fuc–CMCS and Fuc–CMCS@Cur hydrogel beads were characterized by SEM (Fig. 3). The surface of the hydrogel beads displayed folding patterns and depressions, which could be attributed to the dehydration shrinkage of the hydrogel networks during the freeze-drying process (Fig. 3a and d).[34,35] For the microstructure of Fuc–CMCS hydrogel beads, it exhibited minimal wrinkles and folds on the surface. This indicated that polysaccharide-only composition restricted the mobility of water within the hydrogel beads, thereby promoting the formation of a smaller and more compact network structure (Fig. 3a).[36] Upon the incorporation of Cur, the hydrogel bead structure became larger and more wrinkled (Fig. 3d), which was probably attributed to the competitive replacement of Cur with water molecules within the polysaccharide matrix, forming stable hydrogen bonds with the polymer chains. This molecular interaction diminished the water-holding capacity of hydrogel beads, making the water molecules more susceptible to being squeezed out by external forces, thereby yielding a characteristically coarser microstructure. Furthermore, magnification images revealed that all the

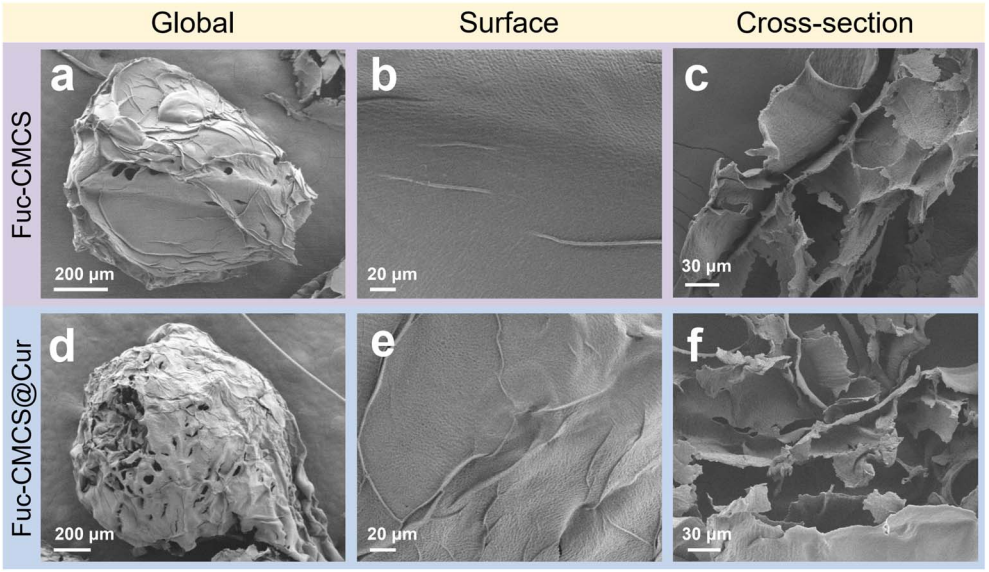

Fig. 3 SEM images of the global (a and d), surface (b and e), and cross-section (c and f) of the Fuc–CMCS hydrogel beads and Fuc–CMCS@Cur hydrogel beads.

hydrogel beads exhibited dense surface structures without any clearly visible micropores and particles (Fig. 3b and e). This suggested that the Cur molecules dispersed well in the hydrogel matrix which could provide superior protective effects.[35] The cross-sectional images showed that both Fuc–CMCS and Fuc–CMCS@Cur hydrogel beads featured a characteristic honeycomb-like network structure (Fig. 3c and f). Nevertheless, a more densely packed pore arrangement within the hydrogel network was observed with the incorporation of Cur. This disparity could be ascribed to the robust hydrogen bonding interactions established between Cur and Fuc–CMCS matrix. These enhanced interactions promoted the development of a more tightly knit and compact hydrogel network.[37]

3.3 The thermal and UV stabilities of Cur encapsulated in Fuc–CMCS@Cur hydrogel beads

Considering the well-documented thermal and photochemical instability of Cur, the stability of Cur within the composite hydrogel beads when exposed to thermal conditions (4, 20, 37, 60, and 80 °C) and UV irradiation ($\lambda = 365$ nm) was examined by closely observing the degradation behaviors of both free and encapsulated Cur. According to Fig. 4a, both free and encapsulated Cur exhibited comparable retention rates without notable influence under mild temperature conditions (4, 20, and 37 °C). In contrast, upon elevating temperatures (60 and 80 °C), hydrogel beads displayed a striking protective advantage in 1 h of storage. We further prolonged the thermal treatment duration to 3 h at 80 °C to evaluate the long-term stability of Cur (Fig. 4b). Free Cur underwent rapid and severe thermal degradation under such conditions, with only approximately 50% of the initial content retained after 3 h of incubation. In sharp comparison, Cur encapsulated within the Fuc–CMCS@Cur hydrogel beads remained at a significantly higher retention level throughout the high-temperature storage. These results clearly validated that the hydrogel bead matrix exerted outstanding protective effects against thermal decomposition of Cur. The improved thermal stability was mainly attributed to the robust physical barrier provided by the polysaccharide network, which effectively isolated Cur from heat-induced degradation. Regarding UV stability (Fig. 4c), free Cur retained only 43.14% of its initial content after 3 h of continuous exposure to 365 nm UV light, indicating severe photodegradation. In contrast, Cur encapsulated in Fuc–CMCS@Cur hydrogel beads exhibited a markedly higher retention rate of up to 84.11%, demonstrating the excellent UV-shielding performance of the hydrogel system. Collectively, these findings confirmed that encapsulation within the Fuc–CMCS hydrogel beads could significantly enhance both the thermal stability and UV resistance of Cur, thereby overcoming its inherent instability against harsh environmental stresses.

3.4 The pH-sensitivity swelling and release behavior of Fuc–CMCS and Fuc–CMCS@Cur hydrogel beads

The equilibrium water content (EWC) and swelling behavior of hydrogels are of great significance in determining the quality of their applications. These properties depend on the interactions and microstructures of the hydrogel networks, which can be used to indicate their physical or chemical crosslinking degrees in suitable solvents.[18,38] As shown in Fig. 5a, Fuc–CMCS hydrogel beads exhibited a higher EWC compared with those encapsulated with Cur, which could be attributed to the ability of Cur to interact with the polysaccharide matrix *via* hydrogen bonds. Acting as a physical crosslinking agent, Cur enhanced the crosslinking degree, thereby decreasing the EWC through competitive molecular interactions. This finding was in accordance with the TGA and SEM results analyzed above.

The swelling behavior of hydrogel beads under varying pH served as a fundamental assessment of their swelling degree and

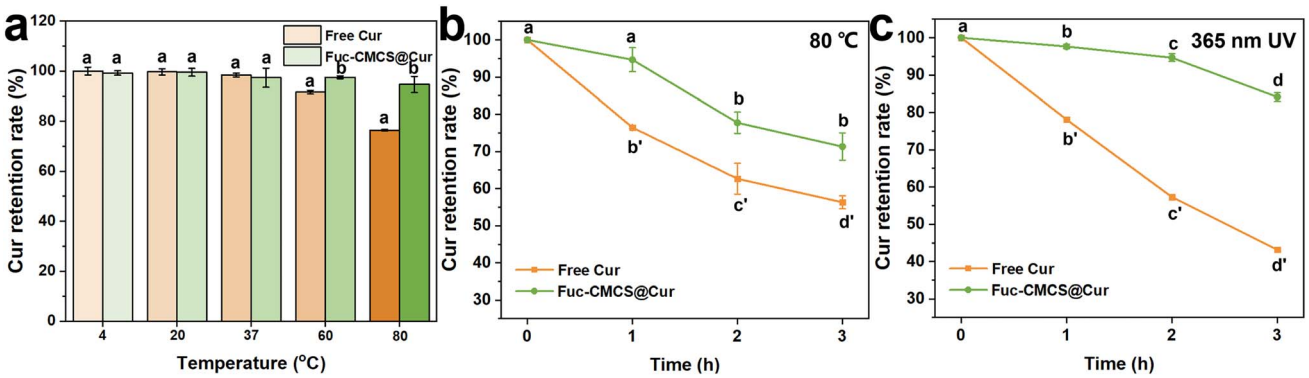

Fig. 4 Cur retention rate of Fuc–CMCS hydrogel beads and Fuc–CMCS@Cur hydrogel beads (a) at different temperatures (4, 20, 37, 60, 80 °C) for 1 h in the dark, (b) at 80 °C for 3 h in the dark, and (c) under 365 nm UV irradiation for 3 h (different letters in the figure represent significant differences at $p < 0.05$).

size change. The freeze-dried hydrogel beads were immersed in medium solutions with different pH values (2.0, 4.0, 6.0, and 7.4) for 4 h to achieve their equilibrium swelling. As shown in Fig. 5b, the swelling degrees of Fuc–CMCS hydrogel beads were higher than those of Fuc–CMCS@Cur hydrogel beads across all pH values. In the absence of Cur, a higher swelling degree and water absorption capacity was observed for Fuc–CMCS hydrogel beads. This could be attributed to its relatively loose networks and the insufficient crosslinking density, consistent with the above discussion.[39] Conversely, upon the addition of Cur, Cur elevated the crosslinking density of hydrogel beads by establishing hydrogen bonds with polysaccharides, which restricted the expansion space of the network structure and consequently decreased the swelling degree. This conclusion was further corroborated by the size change rates of the hydrogel beads presented in Fig. 5c and d. Specifically, across all pH values, the main size change rates of the Fuc–CMCS hydrogel beads were consistently higher than those of the Fuc–CMCS@Cur hydrogel beads. Notably, both Fuc–CMCS and Fuc–CMCS@Cur hydrogel beads demonstrated distinct swelling behaviors as the pH value

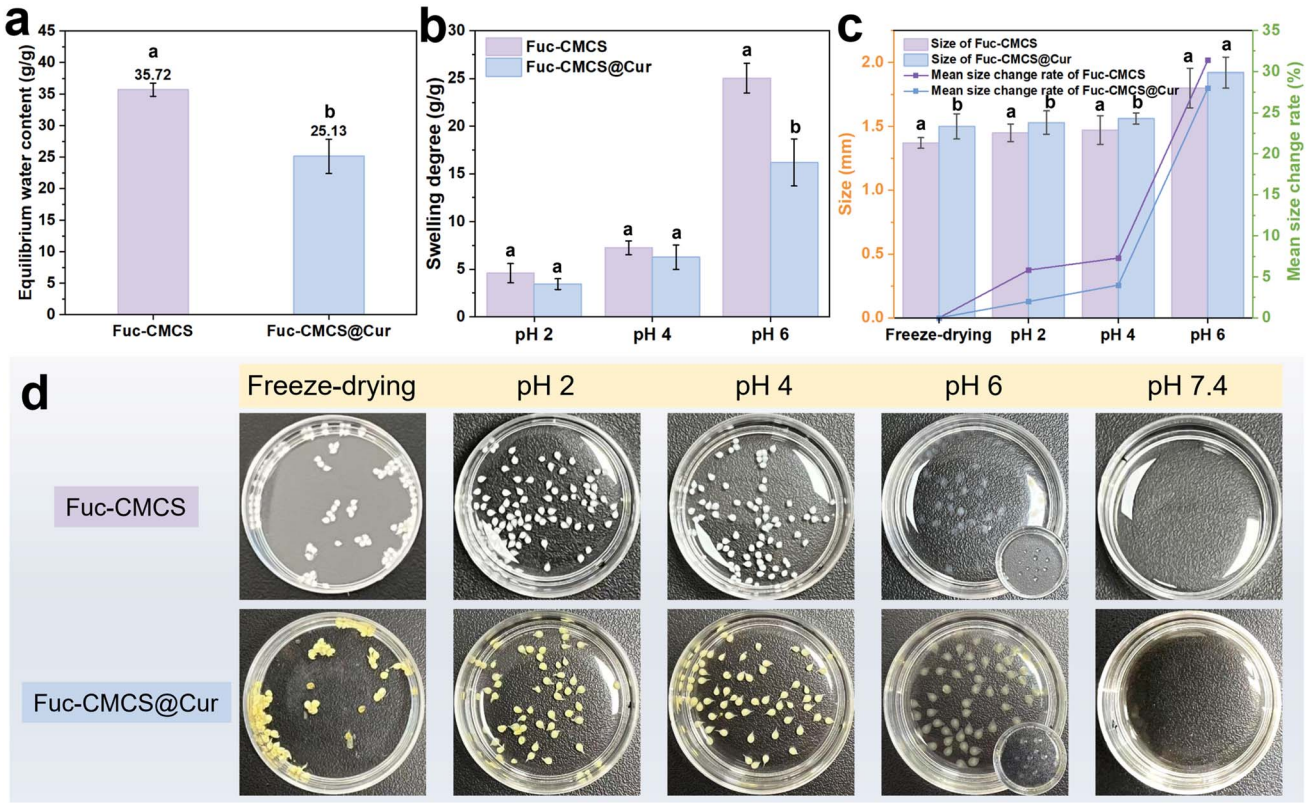

Fig. 5 (a) Equilibrium water content, (b) swelling degree, (c) size and mean size change rate, and (d) appearance of Fuc–CMCS hydrogel beads and Fuc–CMCS@Cur hydrogel beads under different pH conditions (different letters in the figure represent significant differences at $p < 0.05$).

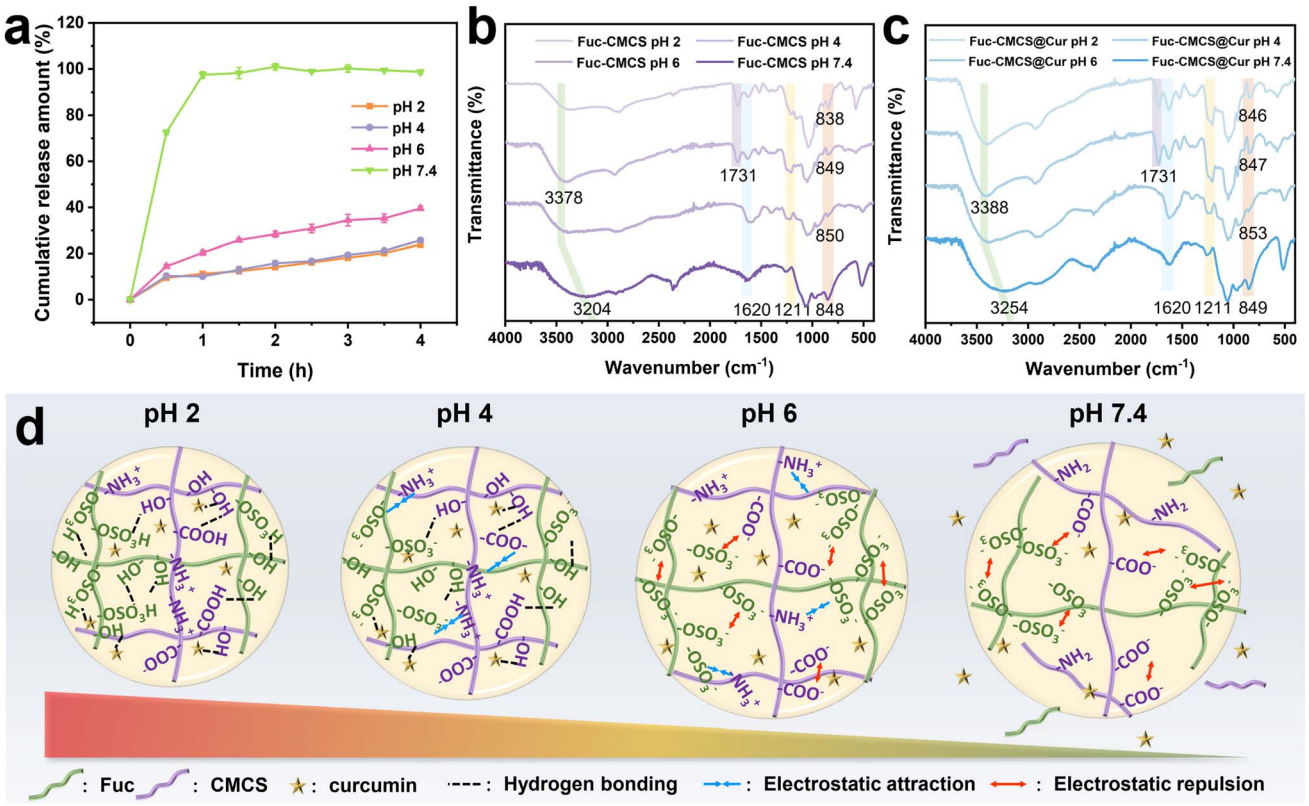

Fig. 6 (a) Cumulative release amount of Cur from Fuc–CMCS@Cur hydrogel beads under different pH conditions; FTIR spectra of (b) Fuc–CMCS hydrogel beads and (c) Fuc–CMCS@Cur hydrogel beads under different pH conditions; and (d) schematic illustrations of the interactions between Fuc and CMCS under different pH conditions.

changed, which revealed the pH-responsive characteristics of these hydrogel beads. The swelling degrees of these hydrogel beads at pH 2.0 and 4.0 were markedly lower compared to those at pH 6.0. Interestingly, when the pH reached 7.4, both hydrogel beads dissolved entirely, making it unfeasible to measure and compare their swelling degrees (Fig. 5d). In an environment with a relatively high concentration of H^+ ions (pH 2.0 and 4.0), the abundance of H^+ ions prompted the protonation of sulfate groups in Fuc and carboxyl groups in CMCS. The protonated groups effectively suppressed electrostatic repulsion while promoting intermolecular hydrogen bonding, causing the matrix to become more compact with no significant swelling. In contrast, in a weak acidic environment (pH 6.0), progressive deprotonation of these functional groups amplified electrostatic repulsion, thereby facilitating network expansion. Subsequently, this expansion enabled greater fluid absorption by the hydrogel beads, manifesting as heightened swelling with larger and more transparent shapes,[32,36] while in an alkaline environment (pH 7.4), the gradual deprotonation of amino groups in CMCS intensified electrostatic repulsion of sulfate groups and carboxyl groups, ultimately leading to the disintegration of hydrogel beads. The obtained results revealed that the hydrogel beads exhibited remarkable pH-sensitivity, making them suitable for application in pH-responsive delivery systems.

To further demonstrate the outstanding pH-sensitivity of the hydrogel beads, the pH-dependent release profile of Cur from the hydrogel beads in medium solutions with different pH values (2.0, 4.0, 6.0, and 7.4) for 4 h was investigated and is illustrated in Fig. 6a. As anticipated, Cur exhibited varying release behaviors in different pH environments. Specifically, the cumulative release amounts of Cur were only 23.84% and 22.37%, respectively, after incubating in the solution media at pH 2.0 and 4.0 for 4 h. Under pH 6.0, the cumulative release amount increased to 39.56% after incubation. This increment could be explained by the significant swelling of hydrogel beads which enabled Cur to be released relatively quickly from the expandable pores of the hydrogel beads. When increasing the pH to 7.4, Cur demonstrated a rapid release behavior and reached 100% release within one hour, due to the disintegration of the hydrogel beads. The above analysis firmly confirmed that the hydrogel beads developed in this study possessed remarkable pH-sensitivity, allowing them to effectively prevent the premature release of the encapsulated Cur in an acidic environment (such as the stomach) and to facilitate a sustained release in a neutral or weakly alkaline environment (such as the intestinal tract).

To investigate the pH-sensitive mechanism of hydrogel beads, the FTIR spectra of Fuc–CMCS and Fuc–CMCS@Cur hydrogel beads after the storage under various pH conditions for 4 h were recorded and are displayed in Fig. 6b and c. The relatively low content of Cur might account for the lack of significant changes in the FTIR spectra after encapsulation.[30] Additionally, a schematic diagram is included in Fig. 6d to provide a visual representation of the pH-sensitivity mechanism

of the hydrogel networks. At pH 2.0, the characteristic peak observed at 1731 cm^{-1} was assigned to the protonated carboxyl groups (–COOH) in CMCS, consistent with its pK_a value of 2.7.[12] Meanwhile, the peak at 838 cm^{-1} corresponded to the C–O–S stretching vibration of protonated sulfate groups (–OSO_3H) in Fuc, whose pK_a ranges from 1.0 to 2.5.[10] Both protonated functional groups could form strong intermolecular hydrogen bonds with hydroxyl moieties present in the polysaccharide chains and Cur molecules. In addition, a distinct peak at 1211 cm^{-1} appeared under acidic conditions (pH < 6.5), which was attributed to the protonation of $-NH_2$ to $-NH_3^+$ in CMCS.[12,24] Simultaneously, the peak at 1620 cm^{-1} was ascribed to the asymmetric stretching of unprotonated carboxylate groups ($-COO^-$), which only accounted for a small fraction at this low pH. At this pH, hydrogen bonding thus acted as the dominant intermolecular force that stabilized the hydrogel bead network. At pH 4.0, the spectral features showed no significant differences from those at pH 2.0, except for the shift of the peak from 838 to 849 cm^{-1} (or from 846 to 847 cm^{-1}). This probably indicated the deprotonation of sulfate groups ($-OSO_3^-$) in Fuc due to its low pK_a. As a result, it might enable electrostatic attraction with $-NH_3^+$ in CMCS. Meanwhile, gradually deprotonated carboxyl groups could also generate such interaction with $-NH_3^+$. Here, the main forces acting on the hydrogel beads comprised hydrogen bonding and electrostatic attraction. At pH 6.0, the disappearance of the peak at 1731 cm^{-1} and the emergence of a broad peak at 1620 cm^{-1} confirmed complete deprotonation of carboxyl groups. At this pH value, the dominant force within the hydrogel beads shifted to electrostatic repulsion between $-OSO_3^-$ and $-COO^-$, leading to significant swelling of hydrogel beads and correspondingly Cur release. Notably, the hydrogel beads demonstrated remarkable structural integrity without disintegration, primarily due to synergistic stabilization through hydrogen bonding and electrostatic interactions between $-NH_3^+$ and both $-COO^-$ and $-OSO_3^-$ groups. At pH 7.4, the peak at 1211 cm^{-1} (representing $-NH_3^+$) completely disappeared, indicating full deprotonation of amino groups. This change intensified electrostatic repulsion between negatively charged $-COO^-$ (from CMCS) and $-OSO_3^-$ (from Fuc), which disrupted the original network structure and ultimately led to the disintegration of the hydrogel beads. Moreover, the broad peak underwent shifts from 3378 to 3204 cm^{-1} (or from 3388 to 3254 cm^{-1}) at pH 7.4, respectively. These shifts differed from those of the pure components (Fig. 2a), suggesting that the hydrogel beads' components still maintained non-covalent interactions such as hydrogen bonds.[10,34]

3.5 Cur release and antioxidant activity

3.5.1 The release of Fuc–CMCS@Cur hydrogel beads *in an in vitro* simulated gastrointestinal environment. The release profile of encapsulated Cur and retention rate of free Cur in simulated gastrointestinal fluids were checked and are illustrated in Fig. 7a and b. After incubation in SGF (pH 2.0) for 2 h, the Fuc–CMCS@Cur hydrogel beads effectively retained the encapsulated Cur, and the cumulative release amount of Cur was less than 20%. This phenomenon could be ascribed to its diminished swelling capacity under acidic conditions. In contrast, the amount of Cur released from the hydrogel beads in SIF (pH 7.0) increased dramatically compared to that in SGF, with approximately 100% of Cur being released within 4 h. The significantly enhanced Cur release kinetics observed in SIF could be mechanistically attributed to the pH-responsive nature and corresponding swelling behavior of the hydrogel matrix at higher pH. Notably, free Cur is highly susceptible to degradation within the human gastrointestinal tract. The controlled release behavior of Cur from the hydrogel beads effectively avoided premature degradation, thereby greatly improving its bioavailability and functional efficacy.[40] As depicted in Fig. 7b, free Cur experienced degradation in both SGF and SIF over a 6 h period, with only 41.77% of the initial amount remaining. These findings demonstrated that the Fuc–CMCS@Cur hydrogel beads not only display pH-sensitive release characteristics but also protect Cur against enzymatic degradation through a polysaccharide matrix shield. Consequently, the encapsulated Cur achieved an almost 100% release amount, ensuring excellent active retention and delivery efficiency. These features were also clearly demonstrated by the insets in Fig. 7a and b, which

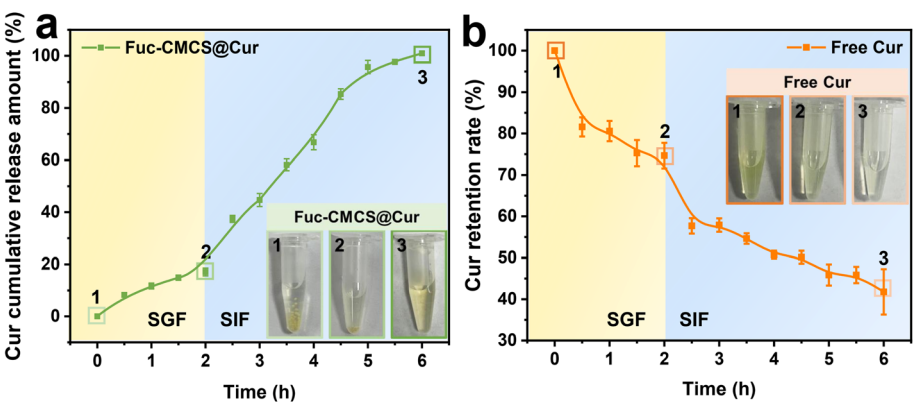

Fig. 7 (a) Cumulative release amount of Cur from Fuc–CMCS@Cur hydrogel beads in simulated digestion fluids (SGF + SIF); and (b) retention rate of free Cur in simulated digestion fluids (SGF + SIF). Insets show the release or retention status of Cur at different stages (1 represents the initial state before treatment, 2 represents the state after completing digestion in SGF, and 3 represents the state after completing digestion in SIF).

vividly showed the release status of free and encapsulated Cur under different medium conditions at various time points.

3.5.2 The antioxidant activity of Fuc–CMCS@Cur during digestion. Although Cur exhibits strong antioxidant properties, free Cur is highly susceptible to degradation within the human gastrointestinal environment, which significantly undermines its antioxidant activity.[40] Herein, EPR spectroscopy was employed to directly quantify *in situ* radical content in DPPH upon contact with Fuc–CMCS@Cur hydrogel beads as a function of time.[41,42] A typical set of time-resolved EPR spectra of DPPH with Fuc–CMCS@Cur hydrogel beads after digestion in PBS (pH 7.4), SGF, and SIF are shown in Fig. 8a–c, respectively. At 0 min, all typical DPPH EPR spectra were observed, with their intensity decreasing over time until the end of the 30 min test. The integrated area of the EPR spectrum, which was proportional to the radical density,[20] was plotted as a function of time (Fig. 8d). Fuc–CMCS@Cur hydrogel beads without gastrointestinal digestion (incubated in PBS) showed a fast decline in DPPH EPR signals over time, with the signal reaching a steady state within approximately 10 min. This rapid radical-scavenging behavior was consistent with the well-recognized strong antioxidant activity of Cur. After digestion in SGF (2 h), the decay rate of the DPPH EPR signal slowed down noticeably. However, the overall percentage of EPR signal reduction within 30 min was only slightly affected, suggesting that the hydrogel matrix effectively shielded Cur from gastric stress and prevented substantial degradation. Following digestion in SIF (4 h), both the decay rate and the final intensity of the DPPH EPR signal were comparable to those of the undigested control in PBS, further confirming that Cur retained excellent antioxidant activity after intestinal digestion. Taken together, these results verified that Fuc–CMCS@Cur hydrogel beads preserved more than 90% of the antioxidant activity of Cur relative to the undigested control (Table 1). The remarkable protective effect was attributed to the physical barrier formed by the polysaccharide network, which effectively insulated Cur from harsh digestive enzymes, acidic environments, and oxidative stress during gastrointestinal transit.

Subsequently, the decay of the DPPH EPR signal over incubation time was fitted in an attempt to obtain quantitative results. The fitting parameters are presented in Table 1. The single exponential decay function was the best fit for the behavior of Fuc–CMCS@Cur treated in PBS and SIF, whereas the biexponential decay function was a more accurate model for the response of Fuc–CMCS@Cur treated in SGF. This discrepancy suggested distinct mechanisms or processes for DPPH radical quenching. Complete release of Cur from Fuc–CMCS@Cur hydrogel beads was achieved in PBS or SIF, leading to homogeneous dispersion throughout the solution. All Cur was in a uniform chemical environment, ensuring equivalent accessibility to DPPH free radicals, thus exhibiting single exponential decay with no significant change in the primary time constant (designated as τ_1). In stark contrast, SGF treatment led to partial release characteristics, where only a minor fraction of Cur became freely dispersed in solution while the majority remained entrapped within the intact hydrogel matrix.

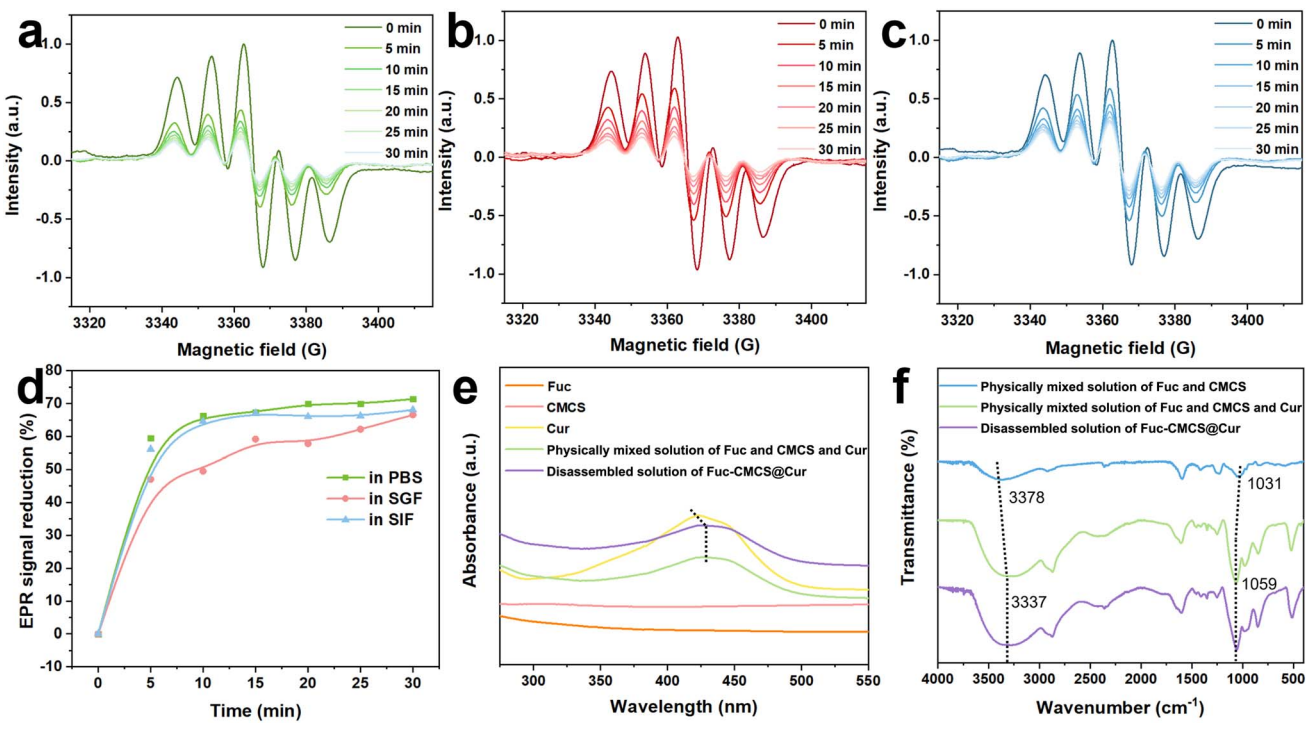

Fig. 8 EPR spectra of DPPH with Fuc–CMCS@Cur hydrogel beads after digestion in (a) PBS, (b) SGF, and (c) SIF, respectively; (d) time dependence of EPR signal reduction of DPPH with Fuc–CMCS@Cur hydrogel beads after digestion in PBS, SGF or SIF; (e) UV-vis spectra of the Fuc, CMCS, Cur, physical mixed solution of Fuc, CMCS and Cur, and disassembled solution of Fuc–CMCS@Cur; (f) FTIR spectra of the physical mixed solution of Fuc and CMCS, the physical mixed solution of Fuc, CMCS and Cur, and the disassembled solution of Fuc–CMCS@Cur.

Table 1 Exponential fitting kinetic parameters of Fuc–CMCS@Cur hydrogel beads after digestion under various conditions determined by the EPR method

Treatment	EPR signal reduction (%)	Maintained antioxidant capacity (%)	τ_1 (min)	Relative amplitude (%)	τ_2 (min)	Relative amplitude (%)	R^2 (%)
In PBS	71.39	100	2.65	100	0	0	99.73
In SGF 2 h	66.55	93.22	0.029	43.31	42.42	56.69	99.37
In SIF 4 h	68.09	95.38	2.75	100	0	0	99.92

This spatial confinement of hydrogel beads for incorporated Cur created differential accessibility for DPPH radicals and correspondingly distinct interaction kinetics between the free and encapsulated Cur fractions, ultimately manifesting as double exponential decay. The secondary time constant (designated as τ_2) exhibited a marked prolongation compared to τ_1, attributable to the extended diffusion period required for DPPH radicals to permeate the dense polysaccharide-based hydrogel matrix prior to accessing encapsulated Cur molecules. Interestingly, the τ_1 value of Fuc–CMCS@Cur treated in SGF was significantly shorter than those in PBS and SIF. This phenomenon probably arose from the fact that Cur released in PBS or SIF continued to interact with the disassembled polysaccharide matrix of hydrogel beads, thereby impeding contact between DPPH free radicals and Cur. Conversely, the hydrogel beads maintained structural integrity in SGF, allowing the released Cur to remain freely dispersed in the solution, which facilitated immediate interaction with DPPH free radicals.

Furthermore, to verify the above analysis, UV-vis and FTIR spectroscopy were employed to characterize the interaction between Cur and the disassembled hydrogel bead polysaccharide matrix. As attested in Fig. 8e, the UV-vis absorption of Cur in the disassembled solution of Fuc–CMCS@Cur hydrogel beads exhibited a red shift compared to free Cur. This finding confirmed the interaction between Cur and the polysaccharide matrix in solution, which was consistent with the physical mixed solution of Fuc, CMCS, and Cur (after excluding the UV-vis absorption interference of Fuc and CMCS). Meanwhile, as shown in the FTIR spectra of Fig. 8f, the broad peak associated with the –OH stretching vibration in the physical mixed solution of Fuc and CMCS shifted from 3378 to 3337 cm^{-1}, and the peak corresponding to the C–O stretching vibration shifted from 1031 to 1059 cm^{-1} upon the addition of Cur, as well as in the disassembled solution of Fuc–CMCS@Cur hydrogel beads. These shifts were attributed to hydrogen bonding interactions between Cur and the polysaccharide matrix.[43] The findings confirmed the interaction between Cur and polysaccharide of the disassembled hydrogel beads, indicating that the polysaccharide matrix could protect Cur in the gastrointestinal environment to some extent even after the hydrogel beads had disassembled in the intestine, thus ensuring sustained bioavailability.

4 Conclusions

This study successfully fabricated pH-responsive polysaccharide hydrogel beads *via* physical crosslinking driven by hydrogen bonding between Fuc and CMCS, which constructed a stable three-dimensional network for Cur encapsulation. Cur served as both a bioactive agent and an additional crosslinker, enhancing the network crosslinking density and structural stability of the hydrogel. The hydrogel beads markedly improved the thermal stability and UV resistance of Cur, and exhibited favorable pH-responsive swelling and controlled release behavior. In simulated gastric fluid, the hydrogel beads maintained a compact structure with low Cur release, whereas nearly complete release was achieved in simulated intestinal fluid. Additionally, after *in vitro* simulated gastrointestinal digestion, the encapsulated Cur retained over 90% of its antioxidant activity, confirming the superior protective performance of the hydrogel beads. This green, food-grade delivery system provides an efficient and sustainable strategy for encapsulation and targeted delivery of labile polyphenolic compounds, addressing critical challenges in their stabilization and controlled release for nutraceutical and supplement applications.

Author contributions

Jiayu Yu: writing – original draft, methodology, investigation, conceptualization. Hongyang Hu: validation, investigation. Yingyi Wang: validation, investigation. Xia Sun: validation, investigation. Hanxu Li: validation, investigation. Shun Xiao: validation, investigation. Bingcan Chen: writing – review & editing, investigation, conceptualization. Hui Li: writing – review & editing, investigation, funding acquisition, conceptualization.

Conflicts of interest

The authors declare that they have no known competing financial interests or personal relationships that could have appeared to influence the work reported in this paper.

Data availability

Data will be made available on request.

Acknowledgements

This work was financially supported by the "Kuang Yaming-Tang Aoqing" Scholars Talents Program from Jilin University (No. 419080524136). The Scientific and Technological Project of Jilin Province of China (No. 20260205034GH). We appreciate Prof. Yanxiong Pan for generously providing the EPR Instrument and helping with EPR spectra acquisition and data analysis.

References

1 Z. Rafiee, M. Nejatian, M. Daeihamed and S. M. Jafari, Application of different nanocarriers for encapsulation of curcumin, *Crit. Rev. Food Sci. Nutr.*, 2019, **59**, 3468–3497.
2 Q. B. Hu and Y. C. Luo, Chitosan-based nanocarriers for encapsulation and delivery of curcumin: a review, *Int. J. Biol. Macromol.*, 2021, **179**, 125–135.
3 L. Q. Zou, B. J. Zheng, R. J. Zhang, Z. P. Zhang, W. Liu, C. M. Liu, H. Xiao and D. J. McClements, Food-grade nanoparticles for encapsulation, protection and delivery of curcumin: comparison of lipid, protein, and phospholipid nanoparticles under simulated gastrointestinal conditions, *RSC Adv.*, 2016, **6**, 3126–3136.
4 G. Y. Kan, L. J. Chen, W. J. Zhang, Q. Q. Bian, X. C. Wang and J. Zhong, Recent advances in the development and application of curcumin-loaded micro/nanocarriers in food research, *Adv. Colloid Interface Sci.*, 2025, **335**, 103333.
5 M. Zhou, F. L. Li, J. Chen, Q. S. Wu and Z. Y. Zou, Research progress on natural bio-based encapsulation system of curcumin and its stabilization mechanism, *Food Sci. Technol.*, 2022, **42**, e78422.
6 T. Thambi, V. H. G. Phan and D. S. Lee, Stimuli-sensitive injectable hydrogels based on polysaccharides and their biomedical applications, *Macromol. Rapid Commun.*, 2016, **37**, 1881–1896.
7 L. Liu, Y. Zhang, S. Yu, Z. Yang, C. He and X. Chen, Dual stimuli-responsive nanoparticle-incorporated hydrogels as an oral insulin carrier for intestine-targeted delivery and enhanced paracellular permeation, *ACS Biomater. Sci. Eng.*, 2018, **4**, 2889–2902.
8 J. H. Fitton, D. N. Stringer, A. Y. Park and S. S. Karpiniec, Therapies from fucoidan: new developments, *Mar. Drugs*, 2019, **17**, 571.
9 S. M. Etman, Y. S. R. Elnaggar and O. Y. Abdallah, Fucoidan, a natural biopolymer in cancer combating: from edible algae to nanocarrier tailoring, *Int. J. Biol. Macromol.*, 2020, **147**, 799–808.
10 Y.-C. Huang, J.-K. Chen, U. I. Lam and S.-Y. Chen, Preparing, characterizing, and evaluating chitosan/fucoidan nanoparticles as oral delivery carriers, *J. Polym. Res.*, 2014, **21**, 415.
11 G. Zhai, Y. Wang, P. Han, T. Xiao, J. You, C. Guo and X. Wu, Drug loaded marine polysaccharides-based hydrogel dressings for treating skin burns, *Int. J. Biol. Macromol.*, 2024, **281**, 135779.
12 X. Lv, W. Zhang, Y. Liu, Y. Zhao, J. Zhang and M. Hou, Hygroscopicity modulation of hydrogels based on carboxymethyl chitosan/alginate polyelectrolyte complexes and its application as pH-sensitive delivery system, *Carbohydr. Polym.*, 2018, **198**, 86–93.
13 N. Wang, J. Tian, L. Wang, S. Song, C. Ai, S. Janaswamy and C. Wen, Fucoidan hydrogels induced by k-carrageenan: rheological, thermal and structural characterization, *Int. J. Biol. Macromol.*, 2021, **191**, 514–520.
14 R. Chang, D. Zhao, C. Zhang, K. Liu, Y. He, F. Guan and M. Yao, PMN-incorporated multifunctional chitosan hydrogel for postoperative synergistic photothermal melanoma therapy and skin regeneration, *Int. J. Biol. Macromol.*, 2023, **253**, 126854.
15 H.-T. Lu, T.-W. Lu, C.-H. Chen, K.-Y. Lu and F.-L. Mi, Development of nanocomposite scaffolds based on biomineralization of carboxymethyl chitosan/fucoidan conjugates for bone tissue engineering, *Int. J. Biol. Macromol.*, 2018, **120**, 2335–2345.
16 H.-Y. Tang, Z. Fang and K. Ng, Dietary fiber-based colon-targeted delivery systems for polyphenols, *Trends Food Sci. Technol.*, 2020, **100**, 333–348.
17 M. Baharizade, S. I. Ghetmiri, M. Mohammady, S. Mohammadi-Samani and G. Yousefi, Revolutionizing knee osteoarthritis treatment: innovative self-nano-emulsifying polyethylene glycol organogel of curcumin for effective topical delivery, *AAPS PharmSciTech*, 2024, **25**, 80.
18 N. Yuan, L. Xu, H. Wang, Y. Fu, Z. Zhang, L. Liu, C. Wang, J. Zhao and J. Rong, Dual Physically Cross-Linked Double Network Hydrogels with High Mechanical Strength, Fatigue Resistance, Notch-Insensitivity, and Self-Healing Properties, *ACS Appl. Mater. Interfaces*, 2016, **8**, 34034–34044.
19 X. Huang, J. Wang, R. Liu, C. Yang, Y. Shao, X. Wang, H. Yi and Y. Lu, An effective potential bifidobacterium animalis F1-7 delivery strategy: supramolecular hydrogel - sodium alginate/tryptophan-sulfobutylether-β-cyclodextrin (Alg/Trp-SBE-β-CD), *Food Hydrocoll.*, 2024, **155**, 110217.
20 H. Li, Y. Pan, Z. Yang, J. Rao and B. Chen, Improving antioxidant activity of β-Lactoglobulin by nature-inspired Cconjugation with gentisic acid, *J. Agric. Food Chem.*, 2019, **67**, 11741–11751.
21 J. H. Muyonga, C. G. B. Cole and K. G. Duodu, Characterisation of acid soluble collagen from skins of young and adult nile perch (Lates niloticus), *Food Chem.*, 2004, **85**, 81–89.
22 P. S. Saravana, S. Karuppusamy, D. K. Rai, J. Wanigasekara, J. Curtin and B. K. Tiwari, Elimination of ethanol for the production of fucoidans from brown seaweeds: characterization and bioactivities, *Mar. Drugs*, 2024, **22**, 493.
23 J. Ge, P. Yue, J. Chi, J. Liang and X. Gao, Formation and stability of anthocyanins-loaded nanocomplexes prepared with chitosan hydrochloride and carboxymethyl chitosan, *Food Hydrocoll.*, 2018, **74**, 23–31.
24 Y. Zhang, W. Zhao, Z. Lin, Z. Tang and B. Lin, Carboxymethyl chitosan/sodium alginate hydrogel films with good biocompatibility and reproducibility by in situ ultra-fast crosslinking for efficient preservation of strawberry, *Carbohydr. Polym.*, 2023, **316**, 121073.
25 Y. H. Lin, H. F. Liang, C. K. Chung, M. C. Chen and H. W. Sung, Physically crosslinked alginate/N,O-carboxymethyl chitosan hydrogels with calcium for oral delivery of protein drugs, *Biomaterials*, 2005, **26**, 2105–2113.
26 M.-C. Lee and Y.-C. Huang, Soluble eggshell membrane protein-loaded chitosan/fucoidan nanoparticles for treatment of defective intestinal epithelial cells, *Int. J. Biol. Macromol.*, 2019, **131**, 949–958.
27 V. K. Pawar, Y. Singh, K. Sharma, A. Shrivastav, A. Sharma, A. Singh, J. G. Meher, P. Singh, K. Raval, A. Kumar,

H. K. Bora, D. Datta, J. Lal and M. K. Chourasia, Improved chemotherapy against breast cancer through immunotherapeutic activity of fucoidan decorated electrostatically assembled nanoparticles bearing doxorubicin, *Int. J. Biol. Macromol.*, 2019, **122**, 1100–1114.

28 G. Huang, Y. Yan, D. Xu, J. Wu, C. Xu, L. Fu and B. Lin, Curcumin-loaded nanoMOFs@CMFP: a biological preserving paste with antibacterial properties and long-acting, controllable release, *Food Chem.*, 2021, **337**, 127987.

29 M. Mohammadian, M. Salami, S. Momen, F. Alavi and Z. Emam-Djomeh, Fabrication of curcumin-loaded whey protein microgels: structural properties, antioxidant activity, and in vitro release behavior, *LWT–Food Sci. Technol.*, 2019, **103**, 94–100.

30 R. Priyadarshi, Z. Riahi and J.-W. Rhim, Antioxidant pectin/pullulan edible coating incorporated with Vitis vinifera grape seed extract for extending the shelf life of peanuts, *Postharvest Biol. Technol.*, 2022, **183**, 111740.

31 K. Liu, X.-Q. Zha, W.-D. Shen, Q.-M. Li, L.-H. Pan and J.-P. Luo, The hydrogel of whey protein isolate coated by lotus root amylopectin enhance the stability and bioavailability of quercetin, *Carbohydr. Polym.*, 2020, **236**, 116009.

32 P. Wang, Z.-g. Luo and Z.-g. Xiao, Preparation, physicochemical characterization and in vitro release behavior of resveratrol-loaded oxidized gellan gum/resistant starch hydrogel beads, *Carbohydr. Polym.*, 2021, **260**, 117794.

33 X. Huang, X. Kou, L. Wang, R. Ji, C. Ma and H. Wang, Effective hydroxylation of tangeretin from Citrus Peel (Chenpi) by edible acids and its improvement in antioxidant and anti-lipase activities, *LWT–Food Sci. Technol.*, 2019, **116**, 108469.

34 X. Chen, H. Liu, Y. Yang, P. Li, X. Wang, K. Zhang, K. Zeng, J. Ming and X. Lei, Chitosan-based emulsion gel beads developed on the multiple-unit floating delivery system for gastric sustained release of proanthocyanidins, *Food Hydrocoll.*, 2025, **159**, 110704.

35 H. Jing, X. Huang, X. Du, L. Mo, C. Ma and H. Wang, Facile synthesis of pH-responsive sodium alginate/carboxymethyl chitosan hydrogel beads promoted by hydrogen bond, *Carbohydr. Polym.*, 2022, **278**, 118993.

36 L. Cao, D. Van de Walle, H. Hirmz, E. Wynendaele, K. Dewettinck, B. V. Parakhonskiy and A. G. Skirtach, Food-based biomaterials: pH-responsive alginate/gellan gum/carboxymethyl cellulose hydrogel beads for lactoferrin delivery, *Biomater. Adv.*, 2024, **165**, 213999.

37 Y. Yang, Y. Liu, S. Chen, K.-L. Cheong and B. Teng, Carboxymethyl β-cyclodextrin grafted carboxymethyl chitosan hydrogel-based microparticles for oral insulin delivery, *Carbohydr. Polym.*, 2020, **246**, 116617.

38 H. Bi, X. Zhang, Q. Wang, Q. Yong, W. Xu, M. Xu, C. Xu and X. Wang, Dynamic reversible disulfide bonds hydrogel of thiolated galactoglucomannan/cellulose nanofibril with self-healing property for protein release, *Ind. Crops Prod.*, 2023, **206**, 117615.

39 C. Zhu, X. Zhang, J. Gan, D. Geng, X. Bian, Y. Cheng and N. Tang, A pH-sensitive hydrogel based on carboxymethylated konjac glucomannan crosslinked by sodium trimetaphosphate: synthesis, characterization, swelling behavior and controlled drug release, *Int. J. Biol. Macromol.*, 2023, **232**, 123392.

40 J. Adiwidjaja, A. J. McLachlan and A. V. Boddy, Curcumin as a clinically-promising anti-cancer agent: pharmacokinetics and drug interactions, *Expert Opin. Drug Metab. Toxicol.*, 2017, **13**, 953–972.

41 D. Sanna, G. Delogu, M. Mulas, M. Schirra and A. Fadda, Determination of free radical scavenging activity of plant extracts through DPPH assay: an EPR and UV-Vis study, *Food Anal. Methods*, 2012, **5**, 759–766.

42 M. Polovka, V. Brezová and A. Stasko, Antioxidant properties of tea investigated by EPR spectroscopy, *Biophys. Chem.*, 2003, **106**, 39–56.

43 Y. Zhang, D. Guo, X. Shen, Z. Tang and B. Lin, Recoverable and degradable carboxymethyl chitosan polyelectrolyte hydrogel film for ultra stable encapsulation of curcumin, *Int. J. Biol. Macromol.*, 2024, **268**, 131616.

